Chapter I.6
An Introduction to Measurements of Atmospheric Composition

Piero Di Carlo

1 Introduction

Measurements of the atmospheric composition could help to improve our understanding of the chemistry, climate changes, deterioration of the urban air quality, dynamics of the atmosphere and to verify theoretical ideas. Atmospheric chemistry involves thousands of species; in Fig. I.6.1, for example, the chemistry of the hydroxyl radical (OH) which is the main oxidant of the troposphere is reported. OH and nitrogen oxides (NO_x) control the formation of the ozone (O_3) which is the main pollutant of the troposphere, through the oxidation of the volatile organic compounds (VOC), carbon monoxide (CO), and methane (CH_4). Direct observations of these species help to understand the fundamentals of tropospheric chemistry and the mechanisms of the formation and evolution of air pollution. Continuous measurements of carbon dioxide (CO_2), collected over the last decades, give the experimental evidence that anthropogenic emissions are forcing changes on the climate, since CO_2 is one of the greenhouse gases. Iodine atoms, at the beginning of the 1990s, have been recognized to play a role in the formation of the ozone hole in stratosphere but no role in the tropospheric chemistry was evident. Very selective observations of iodine oxide in the marine surface boundary layer suggested that it can also have importance in the removal of ozone in troposphere and therefore on air quality (Alicke et al., 1999). An indirect use of the observations of atmospheric composition has been shown by Bertram et al. (2007) studying the dynamics of the upper troposphere, with measurements of NO_x and nitric acid (HNO_3) onboard the NASA DC8 aircraft. They showed that the ratio of NO_x/HNO_3 is a unique indicator of the time that a sampled air mass spent in the upper troposphere after a convention, because HNO_3 is preferentially wet scavenged and its solubility is about 10^8 times higher than NO_x. In the middle of the 1980s English researchers at Halley Bay station in Antarctica observed a reduction of the total column amount of ozone

P. Di Carlo (✉)
Dipartimento di Fisica and Centro di Eccellenza CETEMPS, Universita' di L'Aquila, via vetoio, Coppito L'Aquila, L'Aquila, Italy
e-mail: Piero.Dicarlo@aquila.infn.it

D. Cimini et al. (eds.), *Integrated Ground-Based Observing Systems*,
DOI 10.1007/978-3-642-12968-1_6,

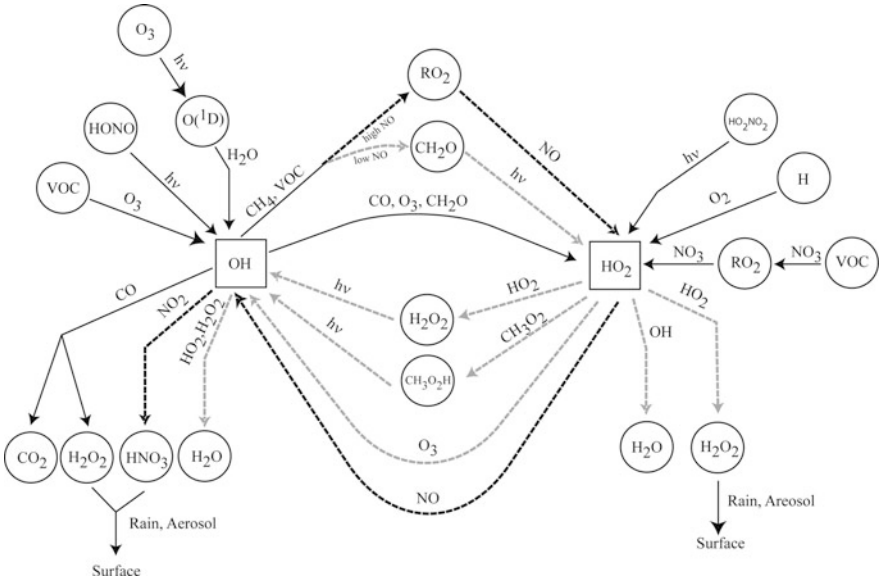

Fig. I.6.1 Schematic view of the main HO_x reactions. Dominant reactions for high NO are marked with *dotted black line*; reactions for low NO are marked with *dotted grey line*. *Black lines* are reactions not influenced by NO concentration

using a ground-base spectrophotometer (Farman, et al., 1985). The spectrophotometer (Brewer) measured the amount of the ultraviolet (UV) light from the sun at five different wavelengths between 306 and 320 nm: they discovered the ozone hole. After confirmations of Farman observations, several theories were proposed to understand the mechanisms of the stratospheric ozone destruction. One of the experiments that unequivocally showed the role of chlorine radicals in the removal of stratospheric O3 was the simultaneous observation of ClO and O_3 onboard the ER-2 aircraft flying inside the polar vortex made by Anderson et al. (1991). O_3 was observed using UV absorption technique, whereas ClO with fluorescence detection of Cl after conversion of ClO through reaction with NO and they showed that as the aircraft flew into the vortex the concentration of O_3 decreased, whereas ClO level increased in comparison with observations outside the vortex: that was the brilliant proof that the chlorine radical is one of the species that destroys ozone during the Antarctic spring months.

Measurement of atmospheric composition is challenging for many reasons. First because we must detect one species in a medium (the atmosphere) where there are thousands of others that can give and interference resulting in incorrect or imprecise observations. Another issue is that the species to be measured are trace gases, in particular those of interest in atmosphere, which have concentrations usually less than a ppm (one part per million). In fact in the atmosphere 99% of the molecules are composed of nitrogen (N_2), oxygen (O_2), and argon (Ar); but the molecules included in that 1% left like O_3, CO_2, nitrogen dioxide (NO_2), ClO are interesting since their concentrations can be modified by human activities and they are involved

in the pollution formation, ozone hole, and climate changes. Two more difficulties in the detection of atmospheric composition arise because temporal and spatial scales are very different from species to species. In Fig. I.6.2 (adapted from Seinfeld and Pandis, 2006) the temporal and spatial scales of the compounds important in atmospheric chemistry are reported. They are grouped into short-lived species (lifetime less than 1 h and spatial scale of 100 m, for example, OH), moderately long-lived species (lifetime from 1 h to 1 year and spatial scale from 0.1 to 1,000 km, for example, NO_x and CO), and finally, long-lived species (lifetime from 1 year to 100 years and spatial scale from hundreds of kilometers to more than 10,000 km, for example, CH_4 and CFCs). Since the temporal and spatial scales are orders of magnitude that differ from species to species, very different instrument techniques are needed to detect species with short lifetime that request fast response instrument compared with long-lived species. The variability of spatial scale implies that some species need to be detected from site to site and eventually using mobile platforms like aircrafts, whereas long-lived species, since well mixed, can be detected only in few sites so that it is not necessary aircraft observation.

Section criteria of instruments for atmospheric composition detection are the selectivity, the detection limit, the accuracy, the precision, and, finally, the mechanical and electrical characteristics like weight, size, power requirement, and autonomy. Selectivity is the instrument specificity of the detection of a given species without interference from other species. Usually systems using optical methods have the advantage that the optical spectra can be used as fingerprint of each species.

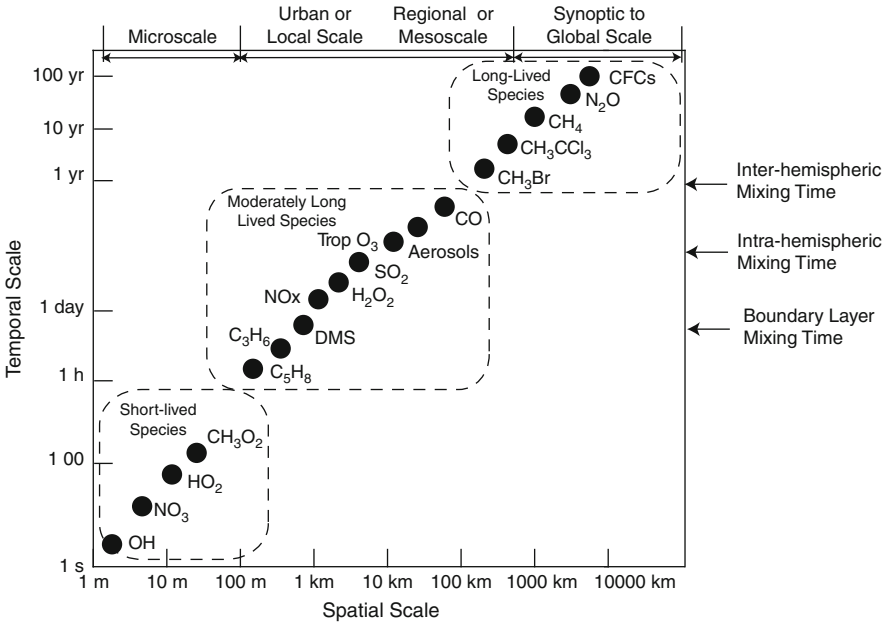

Fig. I.6.2 Spatial and temporal scales of variability for atmospheric constituents (adapted from Seinfeld and Pandis, 2006)

The detection limit is the lowest concentration an instrument can detect. For each compound the detection limit must be significantly lower than the atmosphere concentration, for example, OH concentrations vary in the atmosphere from 0.1 to 1 pptv (parts per trillion) and the detection limit of laser-induced fluorescence systems is 0.001 pptv, whereas detection limit of differential optical absorption spectroscopy instruments is 0.06 pptv, both well below the typical atmospheric level of OH. The accuracy of an instrument is the ability to measure a concentration as close as possible to the real value; this is very important to merge data from global network or from different monitoring stations. The precision is the degree of reproducibility of a measurement under unchanged conditions; this property is required for flux measurements or measurements of concentrations that have to be used to flux retrieval as well as to monitor the long-term trends of a compound. The mechanical and electrical characteristics are very important in the deployment of instruments in remote areas or on platforms like aircrafts where a restrict amount of electrical power and of space is available and there is a limit on the weight of the instrument. In these situations, the design and realization of an instrument with low power consumption, as light and compact as possible, are very important.

A unique technique as well as a unique instrument which are able to detect all the atmospheric species are not available for the motivations above, because each species has its own properties in terms of absorption spectrum, fluorescence wavelength, and so on. Although an "universal" instrument does not exist, a technique to measure as much species as possible is attractive. In this chapter laser-induced fluorescence (LIF) and differential optical absorption spectroscopy (DOAS) techniques will be described, since they can be used to detect several species at the same time or changing some parts of them.

2 Laser-Induced Fluorescence (LIF)

Fluorescence is the emission of light from the relaxation of atoms or molecules from an excited state to a lower electronic state. In the LIF technique the molecules are excited using a laser as light source which emits at wavelengths coincident with the molecular transition from the ground state to an excited electronic state. Molecules after the excitation can lose energy by quenching that converts it into thermal motion of the molecules or by internal excitation of non-fluorescent species. The fluorescence signal is (Wood and Cohen, 2006)

$$S = RQC, \tag{1}$$

where S are counts/s, R the excitation rate, Q the fluorescence quantum yield, and C the collection efficiency of the instrument. The excitation rate is

$$R = E\left\{1 - \exp\left(-cl\int \phi(\nu)\,\sigma(\nu, T, P)\right)d\nu\right\} \tag{2}$$

and approximating $e^{-x} \sim (1 - x)$:

$$R = Ecl \int \phi(\nu)\, \sigma(\nu, T, P) d\nu, \tag{3}$$

where E is the excitation power (photons/s), c the number density of the absorbing species over the path length l, $\Phi(\nu)$ the spectral profile of the excitation source, and σ (ν, T, P) the absorption cross section of the species under detection. The fluorescence quantum yield Q is the fraction of excited molecules that fluoresce:

$$Q = \frac{k_{\text{fluo}}}{k_{\text{fluo}} + \sum_i k_{Qi}\,[M_i]}, \tag{4}$$

where k_{fluo} is the radiative rate constant of the excited species (the inverse of the lifetime τ), k_{Qi} the quenching rate constant due to collision deactivation by bath molecules M_i (mainly nitrogen, oxygen and water vapor) and $[M_i]$ the concentration of the bath molecules. Usually at ambient pressure the quenching rate is much greater than the fluorescence k_{fluo}, so the low pressure in the detection chamber reduces the first (lower bath molecule) that helps to have a bigger fluorescence signal. The collection efficiency, C, is

$$C = \Omega \int T(\nu)\, \eta(\nu)\, \varepsilon(\nu)\, d\nu \int_{t_1}^{t_2} \exp\left(\frac{-t}{\tau}\right) dt, \tag{5}$$

where Ω is the fraction of the fluorescence solid angle intercepted by the collecting lens and focused onto the detector, $T(\nu)$ the transmission through the collection optics, $\eta(\nu)$ the quantum efficiency of the detector, $\Phi(\nu)$ the emission spectrum of the molecule, and the last integral the fraction of fluorescence in the detection time gate t_2–t_1. To calculate all the parameters of the equations above is not easy; it is for this reason that the following equation instead of the relation (1) is used in the LIF technique:

$$S = \alpha \chi, \tag{6}$$

where S is the fluorescence signal in counts/s, α the calibration constant, and χ the mixing ratio of the species to be detected. The calibration constant (counts/s/ppbv) is determinate injecting known amounts of the species in the detection cell of the instrument and measuring the fluorescence as function of the species concentrations. Figure I.6.3 shows the calibration of L'Aquila University LIF system for NO_2 observations. In the calibration the fluorescence signal in terms of counts per seconds is plotted as a function of seven different amounts of NO_2 sent in the detection cell (Fig. I.6.4), the slope of the straight line that fits the observation points is the calibration constant (a) that when substituted in Eq. (6) allows to derive the concentrations from the fluorescence signal.

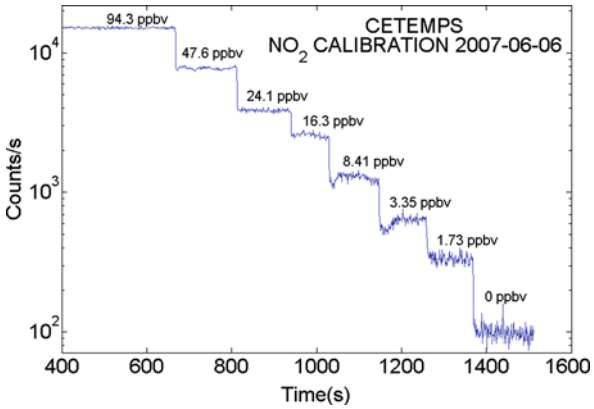

Fig. I.6.3 Example of the increase of the counts/s increases the amount of NO_2 injected in the LIF system of L'Aquila during calibration

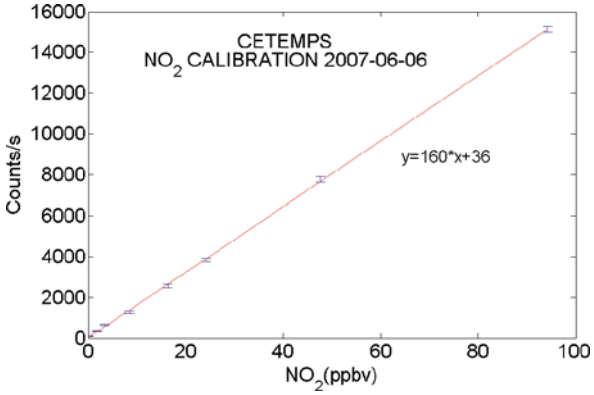

Fig. I.6.4 Fit of the calibration points and equation of the straight line. The slope of this line is the calibration constant used for the LIF concentration measurements

Usually in all kinds of measurements unwanted signals are superimposed at the signal of the species to be detected; they do not give any information and mask the "real" signal. This is the background (B) in the LIF technique, which is due to optical scatter from the surface chamber, Raman, Rayleigh, and Mie scattering, dark current of the PMT, and eventual interference due to fluorescence of other species. The detection limit ($\chi_{\min}$) is the minimum detectable mixing ratio of a species:

$$\chi_{\min} = \frac{\mathrm{SNR}}{\alpha}\sqrt{\frac{2B}{t}}, \tag{7}$$

where $\mathrm{SNR} = St/\sigma_s$ is the signal-to-noise ratio, α the calibration constant, S the fluorescence signal, B the background, t the time interval of the measurements, and σ_s the uncertainty in the fluorescence measurements. In every LIF instrument, fluorescence signal and background are measured and both are very important in determining the detection limit. In Table I.6.1 the detection limits of LIF systems used to detect some important tropospheric species are reported.

Table I.6.1 Detection limit for some tropospheric species measured with LIF systems

Species	Detection limit (pptv)
OH	0.005
HO_2	0.005
NO_2	5
NO	0.07
NO_3	76
N_2O_5	22
ClO	3
$ClONO_2$	10

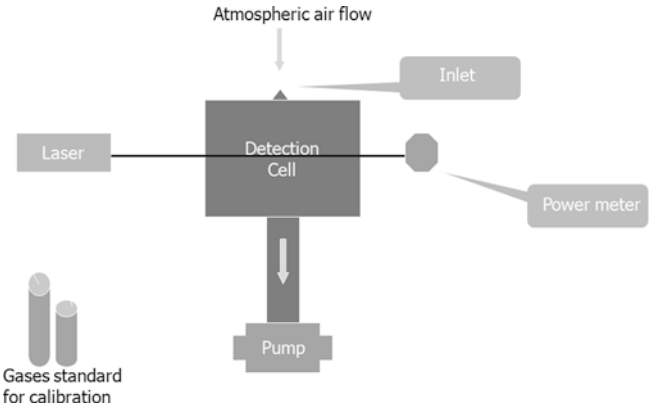

Fig. I.6.5 Sketch with the main parts of LIF system

A schematic view of L'Aquila LIF system is reported in Fig. I.6.5: the main part is the detection cell where the atmospheric air is pulled through a small orifice that is the inlet to be sampled. The air flow is perpendicularly crossed by the laser beam that excites the molecules. Perpendicularly to both air flow and laser beam there is the detection system that includes lens to increase the field of view, interferential filters to cut non-fluorescence light, and the photomultiplier that detects the fluorescence photons. Other important parts of the LIF system are (1) the pump system that takes atmospheric air into the detection cell and keeps it at low pressure to reduce the quenching, (2) the calibration system that for NO_2 instruments includes a cylinder with NO_2 and zero air that will be mixed using a gas-flow controllers to change the NO_2 concentration. For the calibration of the LIF system that measures species like OH a more complicated system is used for real-time OH production since OH which is not stable cannot be stored in cylinders (Faloona et al., 2004), and (3) since the fluorescence is a function of the laser power, the last part of the LIF system is the photodiode that monitors the laser power [see relation (3)]. In Fig. I.6.6 a picture of L'Aquila LIF system is shown and more info about this system is reported in Dari-Salisburgo et al. (2009). The laser is the main part of a LIF system and its emission wavelength has to be selected matching the absorption spectrum of the molecules that must to be detected. In Table I.6.2, the wavelength of the laser used

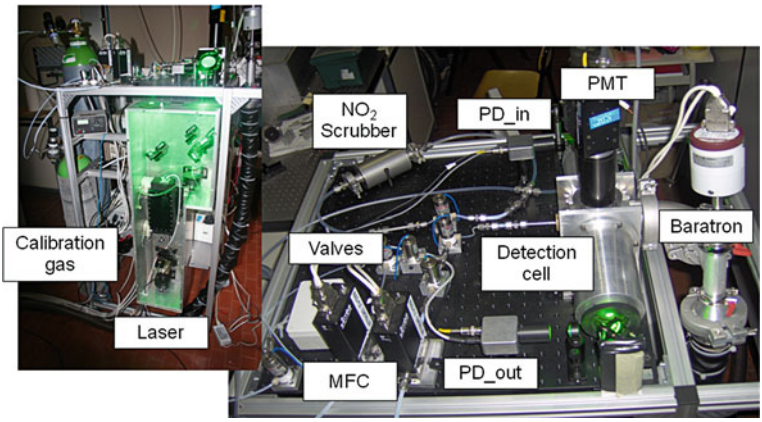

Fig. I.6.6 Pictures of L'Aquila University LIF system for NO_2 measurements

Table I.6.2 Wavelength of lasers used to detect tropospheric species with LIF systems

Species	Laser wavelength (nm)
OH	308
HO_2	308
NO_2	408, 440, 532, 585, 565, 640
NO	226
NO_3	662
N_2O_5	662

for the detection for each species is reported. For NO_2 there are different possible wavelengths, so a variety of lasers can be utilized. It is also worth nothing that HO_2 is not directly detected at 308 nm, but it is indirectly detected measuring the OH produced after the conversion of HO_2 into OH by reaction with NO.

Looking at the expression of the detection limit [Eq. (7)], it is evident that reducing the background signal implies the detection limit is lower so that the instrument is able to detect smaller concentrations. This can be achieved using a time gating, a technique in which the detector (usually a photomultiplier in the LIF) is activated to collect photons only for a period of time. To apply this method a pulsed laser and a low pressure inside the detection cell are required. Pulsed laser is demanded because to reduce the background, the gate will be opened just after the laser pulse since the non-fluorescence signals like Rayleigh and Mie scattering have a time duration similar to the laser pulse. For each pulse (laser pulse in this case is also used as trigger for the gate) the detector is activated until the end of the fluorescence; for example, using a laser at 10 kHz (that gives 10,000 pulses/s) the gate will be opened and closed 10,000 times per second. Opening the gate after the laser pulse excludes most of the non-fluorescence signals and since the fluorescence has a longer time duration it can be detected. The pressure inside the detection cell is kept low (around few

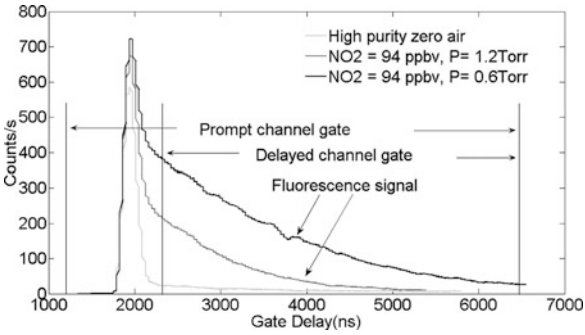

Fig. I.6.7 LIF signals with zero air and with 94 ppbv of NO_2. The fluorescence signal when NO_2 is injected in the detection cell is reported for two different cell pressures. The period in which the gate is open and the photomultiplier detects the fluorescence is signed

Torr) to increase the time duration of the fluorescence; a temporal sketch of the time gating is showed in Fig. I.6.7. The disadvantages of the time gating are the potential surface loss on the pressure-reducing orifice of the inlet (0.3–3 mm of diameter) and the pumps used to reduce pressure that usually are heavy and consume power. Another technique used to reduce the background is to tune the laser emission line on the peak of the absorption cross section of the species to be detected and after the measurements to tune it on one side of the absorption peak to measure the background (Fig. I.6.8). These methods require complicated and expensive lasers with tunable emission wavelengths and a system that controls the tuning.

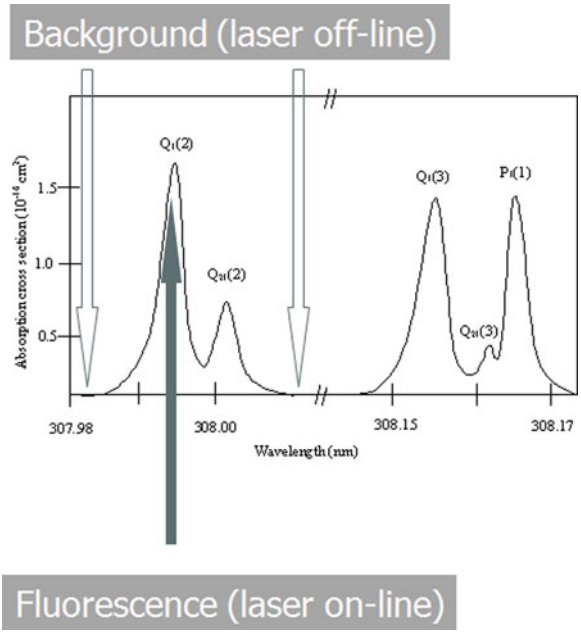

Fig. I.6.8 OH cross section. The *arrows* indicate the parts of the OH spectrum used for the fluorescence detection (laser online) and for the background measurements (laser off-line)

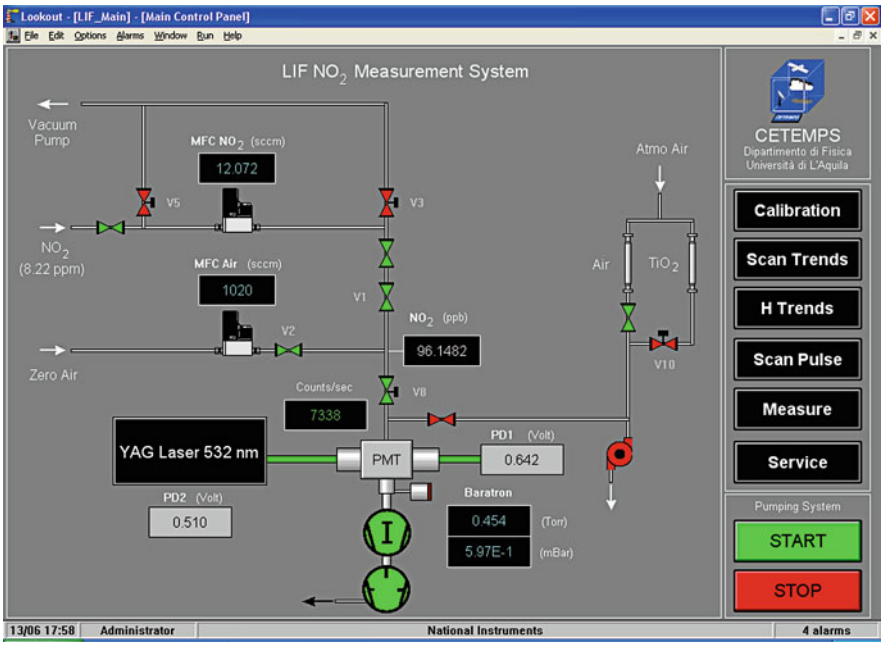

Fig. I.6.9 Picture of the Lookout program developed at the University of L'Aquila to control the NO_2 LIF system

Instruments for atmospheric composition measurements must be able to make continuous observations (24 h a day), sometimes in remote sites or on aircrafts, in some cases, it is not allowed due to the presence of the operator. A completely autonomous instrument must be projected to be used in all the circumstances. In Fig. I.6.9 there is the picture of the control software developed at the University of L'Aquila using LabVIEW and Lookout of National Instrument. This software controls the LIF instrument in all its parts, makes automatic diagnostics, makes automatic calibrations, and allows continuous measurements for several days without the presence of an operator.

In the last decades LIF systems have been used in several ground-base and aircraft campaigns around the world; a detailed list of the campaigns carried out until 2006 can be found in Heard (2006).

3 Differential Optical Absorption Spectroscopy (DOAS)

The absorption of radiation by molecules crossed by lights is described by the Beer–Lambert law:

$$I(\lambda) = I_0(\lambda)\, e^{-L\sigma(\lambda)n}, \tag{8}$$

where $I(\lambda)$ is the intensity of the radiation measured after the absorption, $I_0(\lambda)$ the initial intensity before the absorption, L the pathlength (in cm) where the molecules are crossed by the radiation, $\sigma(\lambda)$ the absorption cross section (in cm^2 $molecules^{-1}$), and n the number density (in molecules cm^{-3}). DOAS technique is mainly used to detect the concentrations of atmospheric molecules and from the expression (8) we have:

$$n = \frac{\log\left(\frac{I_0(\lambda)}{I(\lambda)}\right)}{L \cdot \sigma\,(\lambda)}. \tag{9}$$

The Beer–Lambert law can be used with the simple expression (8) only when one molecule is present and the only interaction between radiation and molecules is absorption. This is not the case of the atmosphere because there are several molecules simultaneously present and also the Rayleigh and Mie scattering that we have to take into account. For the atmosphere, Eq. (8) becomes

$$I(\lambda) = I_0(\lambda) e^{-L\left(\sum_i \sigma_i(\lambda) n_i + \varepsilon^R(\lambda) + \varepsilon^R(\lambda)\right)}, \tag{10}$$

where $\varepsilon^R(\lambda)$ is the Rayleigh extinction coefficient and is equal to $\sigma^R(\lambda) \cdot n_{\text{air}}$ (the first is the cross section of the Rayleigh scattering and the second the concentration of the air) and $\varepsilon^M(\lambda)$ is the Mie extinction coefficient and is equal to $\sigma^M(\lambda) \cdot n_{\text{air}}$ (where the first is the cross section of the Mie scattering). In this case there is the summation over $\sigma_i(\lambda)$ to account for the absorption of all the molecules. The Beer–Lambert law in the form of Eq. (10) is useless to find out the concentration of the molecules, but when Rayleigh and Mie extinctions change slowly as functions of the wavelength the absorption cross section can be written as

$$\sigma_i(\lambda) = \sigma_i'(\lambda) + \sigma_i^S(\lambda), \tag{11}$$

where $\sigma_i'(\lambda)$ is the part of the absorption cross section that changes quickly with wavelength, whereas $\sigma_i^S(\lambda)$ is the part of the absorption cross section that changes slowly with wavelength. Under these hypotheses the relation (10) can be rewritten as

$$I(\lambda) = I_0(\lambda) e^{-L\left(\sum_i \sigma_i'(\lambda) n_i\right)} e^{-L\left(\sum_i \sigma_i^S(\lambda) n_i + \varepsilon^R(\lambda) + \varepsilon^R(\lambda)\right)}, \tag{12}$$

where the first exponential rapidly changes, whereas the second is the slow part of the Beer–Lambert law. Now Eq. (12) can be rewritten in the simple Beer–Lambert form as follows:

$$I(\lambda) = I_0'(\lambda) e^{-L\left(\sum_i \sigma_i'(\lambda) n_i\right)}, \tag{13}$$

where

$$I_0'(\lambda) = I_0(\lambda) e^{-L\left(\sum_i \sigma_i^S(\lambda) n_i + \varepsilon^R(\lambda) + \varepsilon^R(\lambda)\right)}. \quad (14)$$

Equation (14), since it is the part of the cross section that changes slowly multiplied by the emission radiation, is usually calculated with polynomial fit, filter techniques, or FFT (fast Fourier transform) for DOAS using the sunlight or moonlight as source (passive DOAS). It can also be measured in case of active DOAS using laser, lamps, or LED as source.

In Fig. I.6.10 a sketch of a DOAS system is shown; the main parts are: (1) the source that can be a laser when the spectrum of the absorption species is very narrow (for example, OH that absorbs around 308 nm and the spectrum is about 2 pm wide) or a lamp or LED when the absorption spectrum is few nanometers, (2) the spectrometer that has to analyze the absorption spectrum as function of the wavelength to find the fingerprint of the molecule spectrum, (3) the detector that is usually a CCD (charge coupled device), (4) a telescope to collect the absorbed radiation and to collimate light when lamps or LEDs are used as source, and (5) the retroreflector that is usually an array of reflecting prisms fixed some kilometers away from the source and the spectrometer to send back the light after the absorption during the travel in the open atmosphere. In Fig. I.6.11 few picture of the parts of the DOAS system developed at the University of L'Aquila are reported; more details of it can be found in the Di Carlo et al. (2009). The spectral resolution of the spectrometer depends on the source: When a laser is used a very high-resolution spectrometer is needed (less than 0.1 pm) and, in this case, could be helpful for a premonochromator (premono, in Fig. I.6.10) to select the order of the spectrometer and to reduce the unwanted light at wavelengths away from the absorption spectrum of the species under observations. When a broadband source (lamp or LED) is used a small spectrometer, with resolution between 1 and 0.1 nm, is enough. The retroreflector uses

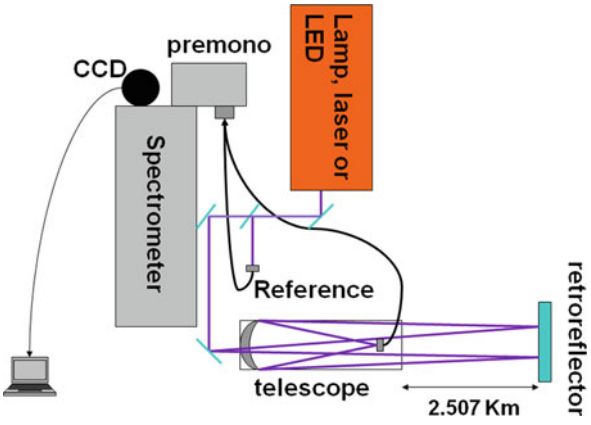

Fig. I.6.10 Schematic view of a DOAS instrument

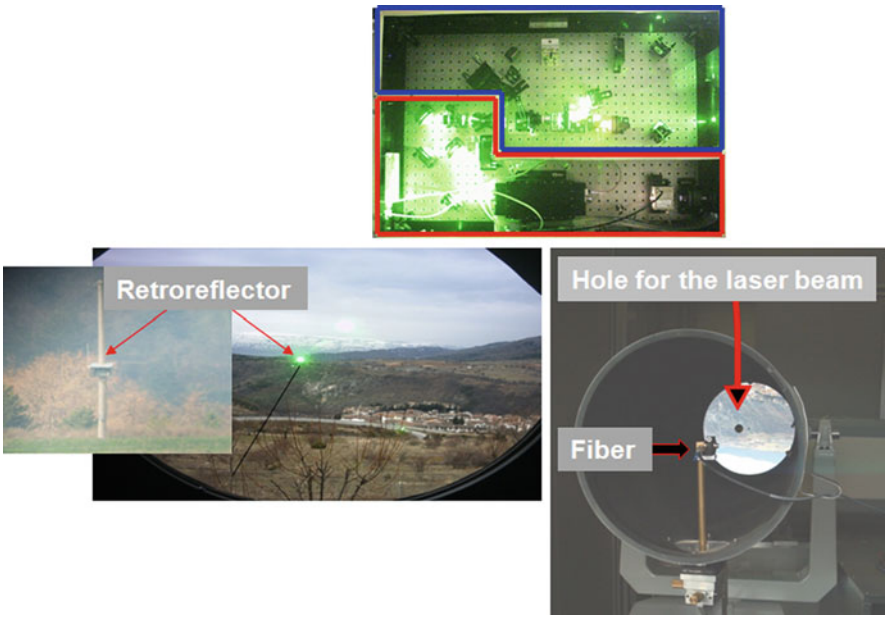

Fig. I.6.11 Pictures of the main parts of L'Aquila University DOAS

an array of prisms instead of a big mirror because it does not need alignment and the configuration with source and spectrometer in one laboratory and the retroreflector at a certain distance allows to double the light path.

Most of the species like ozone, ClO, SO_2, benzene, and toluene absorb in the UV (between 250 and 350 nm), nitrous acid (HONO) and bromine monoxide (BrO) absorb between 300 and 380 nm, NO_2 absorbs between 300 and 500 nm, whereas nitrate radical (NO_3) from 600 to 700 nm. The detection limit of DOAS systems is usually higher than LIF systems: For example, for NO_2 and NO it is 50 pptv, for OH it is 0.06 pptv, for NO_3 it is 0.4 pptv, and for ClO it is 5 pptv. A review of DOAS system can be found in Plane and Sainz-Lopez (2006) or in Platt (1994).

4 Conclusions

LIF and DOAS are optical techniques widely used to observe the atmospheric composition. Usually LIF instruments are smaller and lighter than DOAS and can be used on aircraft platforms. LIF systems allow fast observations so it can also be used for flux measurements and usually data analysis is easier compared to analysis of DOAS data. Looking at the detection limit and selectivity LIF and DOAS are comparable. The big advantage of DOAS systems is that this technique does not need calibration while LIF instruments do. Even if DOAS instruments are usually bigger than LIF, some of them have also been installed on aircraft platforms.

The introduction of LEDs helps to reduce the DOAS instruments size and makes its operation easier compared with those using lamps; the diode laser represents a good opportunity to make cheaper and more compact LIF systems.

Acknowledgments I like to thank G. Visconti, A. D'Altorio, C. Dari-Salisburgo, E. Aruffo, F. Giammaria, F. Del Grande and all the people who helped to develop the LIF and DOAS systems of L'Aquila University.

References

Alicke B, Hebestreit K, Stutz J, Platt U (1999) Iodine oxide in the marine boundary layer. Nature 397:572–573.

Anderson JG, Toohey DW, Brune WH (1991) free-radicals within the Antarctic vortex – the role of CFCS in Antarctic ozone loss. Science 251:39–46.

Bertram TH, Perring AE, Wooldridge PJ, Crounse JD, Kwan AJ, Wennberg PO, Scheuer E, Dibb J, Sachse G, Vay SA, Crawford JH, McNaughton CS, Clarke A, Pickering KE, Fuelberg H, Huey G, Blake DR, Singh HB, Hall SR, Shetter RE, Fried A, Heikes BG, Cohen RC (2007) Direct measurements of the convective recycling of the upper troposphere. Science 315:816–820.

Dari-Salisburgo C, Di Carlo P, Giammaria F, Kajii Y, D'Altorio A (2009) Laser induced fluorescence instrument for NO_2 measurements: observations at a central Italy background site. Atmos Environ 43:970–977.

Di Carlo P, Barone M, D'Altorio A, Dari-Salisburgo C, Pietropaolo E (2009) High-resolution spectrometer for atmospheric studies. J Atmos Solar-Terrestrial Phys 71:1383–1388.

Faloona IC, Tan D, Lesher RL, Hazen NL, Frame CL, Simpas JB, Harder H, Martinez M, Di Carlo P, Ren X, Brune WH (2004) A laser induced fluorescence instrument for detecting tropospheric OH and HO_2: characteristics and calibration. J Atmos Chem 47(2):139–167.

Farman JC, Gardiner BG, Shanklin JD (1985) Large losses of total ozone in Antarctica reveal seasonal Cl0x/NOx interaction. Nature 315:207–210.

Heard DE (2006) Analytical techniques for atmospheric measurements. Blackwell. Oxford, (ISBN 1405123575).

Plane JMC, Saiz-Lopez A (2006) UV-Visible differential optical absorption spectroscopy (DOAS). In: Heard D (ed) Analytical techniques for atmospheric measurements. Blackwell. pp 147–188.

Platt U. (1994) Differential optical absorption spectroscopy (DOAS). In: Sigrist MW (ed) Air monitoring by spectroscopy techniques. Wiley, London, pp 27–83.

Seinfeld JH, Pandis SN (2006) Atmospheric chemistry and physics: from air pollution to climate change. Wiley. New York, NY.

Wood EC, Cohen RC (2006) Fluorescence methods. In: Heard D (ed) Analytical techniques for atmospheric measurements. Blackwell. Oxford. pp 189–228.